

## Article

# Development and Validation of a Novel Surface Defect Index (SDI) Method for the Effective Quality Evaluation of Concrete Surfaces

Fatima Zohra Badi <sup>1</sup>, Salah Eddine Bensebti <sup>1</sup>, Abdelhafid Chabane <sup>1</sup>, Cherif Belebchouche <sup>1,\*</sup> , Tien Tung Ngo <sup>2</sup>, El Hadj Kadri <sup>2</sup> and Slawomir Czarnecki <sup>3,\*</sup> 

- <sup>1</sup> Materials and Durability of Constructions Laboratory, Faculty of Sciences of Technology, University of Constantine 1 Mentouri Brothers, Constantine 25000, Algeria; s\_bensebti@yahoo.fr (S.E.B.)
- <sup>2</sup> Mechanics and Civil Engineering Materials Laboratory (L2MGC), University of CY-Paris, Cergy-Pontoise, 95031 Neuville-sur-Oise, France
- <sup>3</sup> Department of Materials Engineering and Construction Processes, Wrocław University of Science and Technology, Wybrzeże Wyspińskiego 27, 50-370 Wrocław, Poland
- \* Correspondence: cherif.belebchouche@umc.edu.dz (C.B.); slawomir.czarnecki@pwr.edu.pl (S.C.)

**Abstract:** Concrete defects have a significant impact on concrete constructions. These defects should be considered not only aesthetic defects but also structural defects. In this study, a novel Surface Defect Index (SDI) method was developed to quantify the defect volume according to liquids' penetrating properties by applying ready-mixed plaster (RMP). The SDI refers to the volumetric proportion of all apparent and unapparent defects in a given area of concrete, and it is expressed as a percentage of the total volume affected by defects. The proposed SDI method was validated and tested under various controlled defect configurations. Regardless of the specific characteristics of each defect configuration, the SDI method consistently demonstrated a high level of consistency, repeatability, and reproducibility, with coefficients of variation (CV<sub>r</sub> and CV<sub>R</sub>) below 5% and with correlation coefficients of  $R^2 = 0.9968$ . The method succeeded in assessing the surface quality levels through the SDI, demonstrating a significant correlation between this index and the volume of defects. The proposed index was tested on real concrete surfaces, affirming its efficacy in accurately quantifying the volume of surface defects; thus, it can provide an important metric for quality control. Moreover, it provides an excellent evaluation of the quality of concrete surfaces.

**Keywords:** defect volume; SDI; quality of concrete surfaces; ready-mixed plaster (RMP); controlled samples



**Citation:** Badi, F.Z.; Bensebti, S.E.; Chabane, A.; Belebchouche, C.; Ngo, T.T.; Kadri, E.H.; Czarnecki, S. Development and Validation of a Novel Surface Defect Index (SDI) Method for the Effective Quality Evaluation of Concrete Surfaces. *Appl. Sci.* **2024**, *14*, 3828. <https://doi.org/10.3390/app14093828>

Academic Editor: Andrea Carpinteri

Received: 4 April 2024  
Revised: 19 April 2024  
Accepted: 23 April 2024  
Published: 30 April 2024



**Copyright:** © 2024 by the authors. Licensee MDPI, Basel, Switzerland. This article is an open access article distributed under the terms and conditions of the Creative Commons Attribution (CC BY) license (<https://creativecommons.org/licenses/by/4.0/>).

## 1. Introduction

Characterizing the quality of a concrete surface is a major problem for the concrete industry. Surface quality varies depending on the application envisaged for concrete. The surface needs to be not only visually appealing but also structurally sound. Quantifying surface defects is essential for ensuring material quality and durability, and it is equally crucial to understand how these surfaces initially form and how they may be altered. Surfaces may indeed evolve freely during their solidification, but they may also incur damage, or they may take on a closed shape due to the wall effect when in contact with formwork [1,2]. In assessing the severity of surface defects in concrete, it becomes evident that the gravity of these imperfections is not solely determined by the area that they occupy on the surface but also by their depth. Deeper defects can have a more profound impact on the structural integrity and performance of concrete [3,4]. Additionally, the depth of defects can influence their potential to accumulate contaminants and facilitate the growth of microorganisms that might compromise the material's long-term durability [5,6]. Therefore, for aesthetic and functional considerations, the combination of both surface area and depth

provides an objective assessment of concrete surface quality. Surface quality evaluation tends to be subjective and, hence, more difficult, as current specifications allow for visual evaluation, which can lead to disagreements in the detection and evaluation results [7]. The primary quality inspection methods for concrete surfaces are based on manual inspection—size measurement, counting, and classification of bugholes on the surface of concrete [8–10]. The Quality Surface Index (QSI) serves as an illustrative example of a simplified method for evaluating the surface area occupied by pores. This approach, as depicted in Figure 1, which provides a visual representation of this surface evaluation method, involves analyzing pore groups based on their diameter [11]. The sand patch method, according to Kaufmann, involves a pre-defined amount of sand to be applied on the surface to be measured, and it is distributed evenly in circular movements [12].

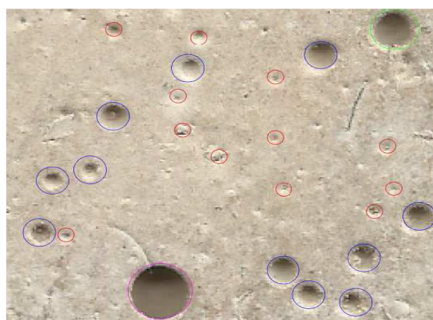


**Figure 1.** Data collection scheme and example using the Quality Surface Index (QSI) approach: Each colored circle represents a specific pore diameter [11].

Despite the fact that manual evaluation is a powerful inspection tool and plays a significant role in detecting and evaluating the quality of concrete, several limitations have been found. First, manual inspection methods are performed by inspectors walking along the surface of a structure while using only their naked eye. It has also been pointed out that large quantities of concrete are widely used. Secondly, the results are not always reliable and are even prone to errors, the process of inspection is time-consuming, and the requirement of experienced inspectors exacerbates the pressing shortage of a highly skilled inspection workforce in the construction industry [10].

As such, the main disadvantage of visual inspection is that it is time-consuming, labor-intensive, and impractical [9,13]. A person's ability to judge faults is limited in that it cannot quantify the value of a given defect. Subjective evaluation depends on individual experience and differing perceptions without a uniform standard; in fact, the same person might even make different judgments on different days. Moreover, it is not possible for a person to determine all possible defects [14]. This technique, however, is extremely laborious and is incapable of representing surface quality [7]. Therefore, this method was replaced with an improved method recommended by the Concrete International Board (CIB) [15], which proposed the comparison of actual concrete surfaces with photographs of reference samples representing seven scales with different degrees of bughole coverage. An illustration of the reference photos is provided in Figure 2. While comparison with a reference sample is a simple avenue to evaluate surface quality, some of the views expressed in that connection assert that it can be problematic because of the variation between the different printed scales of the reference samples and human eyes. Moreover, one surface may have several types of bugholes together or a combination of several different surface imperfections, so using the references becomes difficult and somewhat subjective [14,16–18].

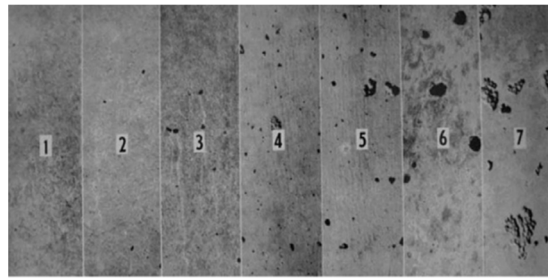


**Figure 2.** Bughole scale(CIB): Comparison of bughole percentages across Surfaces 1 to 7, with Surface 1 having the lowest percentage of bugholes, while Surface 7 has the highest percentage of bugholes [19].

Due to these quantitative problems, more objective detection and evaluation methods have been developed. Image processing technology (IPT) is considered a powerful automated tool for application in to civil engineering materials that can deliver objective results in many areas of study [20,21], such as in concrete bridge inspection [22], the classification of radar images [23], and crack monitoring and quantification for concrete surfaces [24].

There are several methods focused on the use of image processing technology to detect and evaluate the bughole distribution on concrete surfaces [5,10,25–28]. These methods allow one to delineate and quantify areas with surface defects according to the preset quality parameters introduced into the control software [11]. However, there are several deficiencies associated with the direct use of image processing technology for surface defect inspection. Although these methods reduce the subjectivity of the results with image processing algorithms that are designed to assist inspectors in detecting defects, their final results depend heavily on human judgment [29]. In addition, the technical variables for each concrete element (luminosity, brightness, roughness, geometry, etc.) must be correctly analyzed before they are introduced to obtain results that correspond to reality, which impedes their application [11,30]. The detection results of image processing algorithms may be inexact due to the impact of noise, such as illumination, shadows, and combinations of several different surface imperfections [31–34]. Finally, these methods frequently involve the need for several steps; most of them can be repeated on several occasions until the desired results are obtained (trial and error). In other methods, analysis and inspection are more complicated, as in the one method proposed by Majchrowski et al. [18], where an advanced 3D scanner and an optical method were used to analyze and measure the surface topography of a concrete surface. In recent years, other inspection methods were developed based on deep learning algorithms [35]. Deep learning algorithms have demonstrated outstanding technical capabilities in the analysis of inspected images [36–39]. In deep learning, convolutional neural networks (CNNs) are specially constructed to treat the variability in 2D forms. As such networks prevent the complex preprocessing of an image, it is shown that they surpass all other techniques. These characteristics make CNNs an effective identification method that is widely used [29,35,40,41]. These methods find widespread use in the detection of concrete surface cracks [42–46] and bugholes on concrete surfaces [9,18]. However, errors may occur during image tests when there are several types of defects, including cracks, bugholes, and color differences. Thus, it becomes challenging to make a clear distinction between bugholes and some areas of darker color difference, which causes a misunderstanding coming from some similarities in their form. Additionally, due to the light color of bugholes with a small depth, the contrast of colors with the concrete surface is not evident [36,43] because they are usually darker than the remaining concrete surface. While many methods offer benefits in evaluating concrete surfaces, an assessment of the quality of concrete surfaces cannot be provided in a simple manner on-site and by non-specialized operators. Also, previous studies have not considered the case in which there are many different surface defects on the same concrete surface. However, this situation occurs frequently on concrete surfaces. Moreover, these methods face limitations in terms of cost, complexity, time requirements, resolution constraints, and

subjectivity. Additionally, variations in the complexity of defects pose challenges for precise measurements and effective evaluation.

The main purpose of this study is to develop a novel Surface Defect Index (SDI) method for defect quantification. The proposed index is intended to quantify the percentage of the volume occupied by all types of defects found simultaneously on the same surface, regardless of the complexity of their shape and size, using the properties of liquid penetration. Furthermore, the developed method is used for the quantification of randomly distributed defects and the non-uniform distribution of their surfaces and depths, thus enhancing objectivity in surface quality evaluation. This novel method mainly focuses on assessing the impacts of volume parameters (length, width, and depth) on the quality of concrete surfaces. This is because the volume of defects can significantly impact the ingress of harmful elements, such as moisture, aggressive chemicals, and microorganisms, into the concrete matrix. Deeper defects allow pathways for these detrimental elements to penetrate deeper into the concrete, potentially compromising its structural integrity over time.

Therefore, accurately quantifying the volume of defects is essential for identifying potential areas of vulnerability in concrete structures and implementing appropriate maintenance and repair strategies to enhance their long-term durability and performance. The efficacy of the method presented was validated using controlled samples, and it demonstrated successful application and effectiveness when implemented on real concrete surfaces.

## 2. Proposed Method for Quantifying and Classifying Defects in Concrete Surfaces

The surface of concrete generally has many surface defects. These defects should be considered not only as aesthetic defects but also as structural defects that reduce the structural performance and durability of concrete surfaces. A quantitative and simple method for quantifying the defect volume is preferable for the evaluation of the quality levels of concrete surfaces.

The aim of this research was to innovate and develop a method for supporting the objective evaluation of the quality of concrete surfaces. Therefore, an overall evaluation of quality requires the integration of a maximum of parameters. This objective evaluation reduces the discrepancies in quality evaluations. Consequently, we had the challenge of developing a method of evaluating of the level of defects to support the objective judgment of concrete surfaces' quality. The proposed method can quantify the values of all types of defects. Moreover, it is able to reveal all their positions and their infiltration into concrete, especially in the case of large surfaces, by establishing a quantitative survey of defects in terms of the area affected and the depth of the defects.

The developed method is based on the quantification of the volume of defects on the concrete surfaces using concrete's absorptive properties. This is a quantification of surface defects through fluid penetration. The mass transport of fluids in hardened concrete refers to the ability of concrete, once it has cured, to allow the movement of liquids through its structure [47,48].

The capacity of concrete to absorb or take in a liquid varies depending on the concrete mix, its rheological properties, the degree of compaction, and the porous structure of the material [49,50]. Furthermore, the penetration of liquids is a valuable and distinctive property that provides insights into the volumetric fraction of defects that are available for the transport of liquids through the structure of concrete when exposed to liquids. The porosity of concrete, which is determined by the size and distribution of its pores, has a significant impact on the transport of fluids across concrete surfaces. This mass transport characteristics are influenced not only by the presence of defects and their geometry but also by the extent to which these defects have infiltrated into the concrete [51,52]. Thus, quantification of the defect volume in concrete constitutes a key factor in determining the concrete's durability and resistance to degradation. The larger the surfaces of defects and the more profound they are, the greater the potential for water, air, or harmful chemicals to penetrate and cause damage over time. Measuring the volume of surface defects can serve as a valuable indicator in quality control and manufacturing processes, as it can help

identify defects that may affect the performance or appearance of concrete surfaces. A simple measurement method is needed to quantify defects distributed on a concrete surface.

The proposed method uses concrete's property of fluid penetration by applying ready-mixed plaster (RMP) on a concrete surface. The amount of RMP that penetrates through a specific area of the concrete surface reflects the extent of damage in that area by quantifying the volume of the defects that are present; detailed surface information that can be an important parameter in the explanation of the affected proportion of the surface and can provide quantitative information on its quality is captured.

### 3. Principles of the Surface Defect Index (SDI) Method

The procedure implemented in the SDI method includes determining the area to be examined using a frame that specifies this region. This frame serves as an indicator for identifying and isolating the precise portion of the surface under scrutiny, allowing for a focused and systematic assessment of the targeted areas. By defining the boundaries of the analysis zone, the frame facilitates accurate measurements of the volume of defects, ensuring consistency and reliability in the results obtained. Furthermore, it enables the precise evaluation of the level of surface defects, further enhancing the accuracy of the assessment.

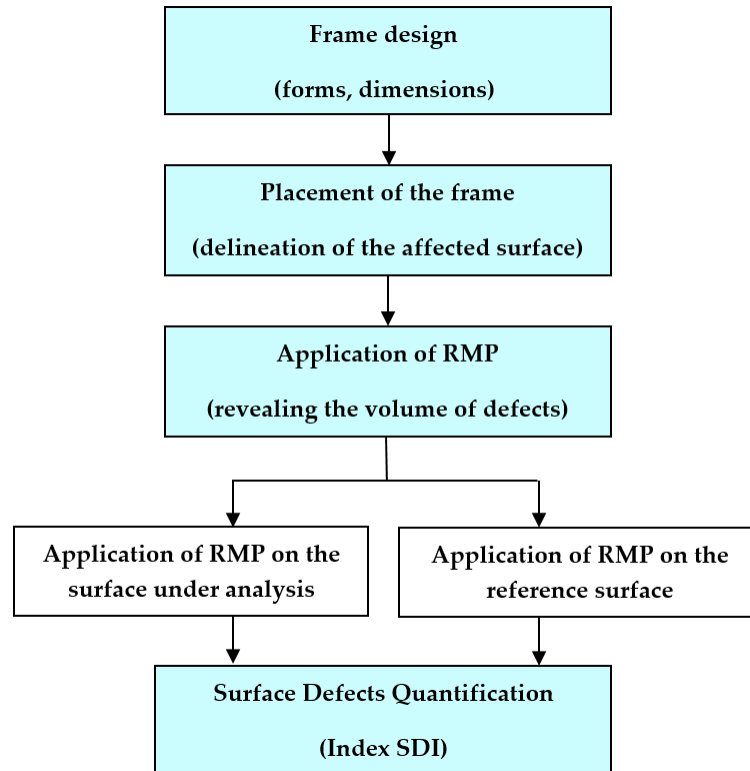
The frame used to determine the surface defect area in this method is not standardized, meaning that there are no fixed or standardized dimensions for its measurements. Indeed, we can adjust the dimensions of this frame according to the specific needs of each sample or analysis. This flexibility allows the accurate targeting and quantification of surface defects by adapting the frame to the unique characteristics of each situation. Thus, we are able to obtain more precise and representative results by considering the variability in volume parameters, which are reflected by the three-dimensional measurement of surface defects, including their length, width, depth, and distribution within the material. Additionally, there is the flexibility to use more than one frame, allowing for a comprehensive assessment of surface defects across different areas or sections of the surface being studied. This approach enables us to capture a more complete picture of the surface characteristics and obtain accurate measurements of defect areas.

Figure 3 describes the overall process of the new method proposed here. The SDI method first accurately delineates the surface defect area and then characterizes the present defects by quantifying their volume (length, depth, and width).

The SDI method was developed using a four-step methodology, which is described in the following:

- The first step in the SDI method, frame design, involves creating a frame adapted to the dimensions of the surfaces under analysis. This frame can be constructed from metal, plastic, or any other rigid material. Its dimensions are adjusted based on the size of the samples and the specific requirements of the study. The role of the frame as a crucial tool is to precisely delineate the measurement area for surface defects in the SDI method.
- In the second step, the placement of the frame for optimal evaluation, it is recommended to position the frame horizontally on the surface being analyzed, ensuring direct contact with the sample surface. This arrangement allows for the precise and effective delineation of the entire affected surface.
- In the third step, the application of RMP, a ready-mixed plaster (a pre-blended mixture of gypsum) was used for the tests to reveal the volume of defects present on the surface. This step involved applying RMP inside the frame at the interface between the frame and the surface under analysis, as well as applying the RMP on an ideal reference surface unaffected by defects (free from defects), which served as a baseline for comparison. The ideal surface was an estimation of the surface under analysis before the damage occurred.
- In the fourth and last step, surface defect quantification, after enclosing the entire damaged area within the frame (a rectangle bounding the length, width, and depth), all present defects were assessed by quantifying their volume. The surface defect

quantification relied on the difference between the measurement obtained from the RMP applied on the surface under analysis and that applied on the reference surface. The quantification of the volume of surface defects is expressed by the Surface Defect Index (SDI), which represents the percentage of defects by volume.



**Figure 3.** Schematic diagram of the steps of the SDI methodology.

## 4. Materials and Methods

### 4.1. Materials

#### 4.1.1. Frame

In this study, a rectangular steel frame with dimensions of 25.8 mm × 16.2 mm and a thickness of 2.7 mm was designed to assess the surface under analysis. The inner dimensions of the frame, which encompassed the affected surface, were 20 × 10.4 cm<sup>2</sup>.

These frame dimensions were chosen based on the surfaces under study. The selection of these dimensions was deliberate, aiming to ensure adequate coverage of surface defect areas while maintaining a practical and manageable size for laboratory use. This size was determined considering the variability in sizes and shapes of the samples to be analyzed, providing a wide enough area to encompass defects of variable sizes. Furthermore, the 2.7 mm thickness of the frame was chosen to ensure adequate rigidity while minimizing any deformation that could skew the measurements. This robust frame design ensured precise delineation of the surface defect measurement area, thereby providing reliable results in assessing the surface quality of the samples.

#### 4.1.2. Ready-Mixed Plaster

Ready-mixed plaster offers excellent penetration properties, in addition to several benefits, such as being safer, cost-effective, and environmentally friendly. Ready-mix plastering provides a convenient and easy-to-use option. In this study, Algerian-made ready-mixed plaster was used, with water comprising 50% of the plaster's weight. The physical and chemical properties of the plaster used are detailed in Table 1.

**Table 1.** Physical and chemical properties of the plaster.

Compounds	SO <sub>3</sub>	CaO	SiO <sub>2</sub>	Fe <sub>2</sub> O <sub>3</sub>	Na <sub>2</sub> O	K <sub>2</sub> O	MgO
(%)	38.44	28.16	10.12	0.34	0.04	0.23	1.25
Density = 2.31							
Setting time = 25 min							

#### 4.2. Experimental Methodology

The procedure employed in the SDI method involved several basic phases. Firstly, before each operation, it was necessary to prepare the tested surface to ensure the perfect penetration of the ready-mixed plaster (RMP). This initial phase involved cleaning the surface by brushing to remove all pulverulent compounds contained in the surface parts. Next, a tray comprising a receptacle containing the RMP and tools needed for the handling process (scraper, cloth) was weighed ( $M_{t \text{ before}}$ ), as shown in Figure 4.

**Figure 4.** Measurement of the RMP and materials used in the study.

The frame was then placed on the surface of the controlled sample to be tested, and the RMP was applied inside the frame with a scraper at the interface between the surface of the frame and the specimen surface ( $20 \times 10.4 \text{ cm}^2$ ), which represented  $208 \text{ cm}^2$  of the total area inspected. This process involved applying a bottom layer using a scraper with sufficient RMP and adequate pressure to ensure their good penetration at the base and to adequately cover all surface defects. Then, the frame was filled with RMP up to its edges (See Section 5.3).

The RMP covering the surface was levelled using a scraper by shaking it periodically from one side to the other, distributing the RMP evenly along the surface frame/specimen surface interface. After the delineation of the RMP on the surface, the edges of the frame were wiped with a cloth to recover any RMP that was deposited during the application process. Once the plastering operations were completed, the cloth and the scrapers were automatically returned to their location in the tray. The tray was then weighed to determine the mass of the RMP deposited at the interface of the frame and specimen surface ( $M_{t \text{ after}}$ ).

The mass of the RMP was determined as follows:

$$M_p = M_{t \text{ before}} - M_{t \text{ after}} \quad (1)$$

The mass of RMP that penetrated into the surface defects ( $M_{pp}$ ) was calculated by weighing the RMP mass deposited at the interface of the frame and specimen surface ( $M_p$ ) relative to the initial mass of the RMP ( $M_0$ ) applied inside the frame on a flat glass surface that was smooth and free of defects (reference medium), as shown in Figure 5.

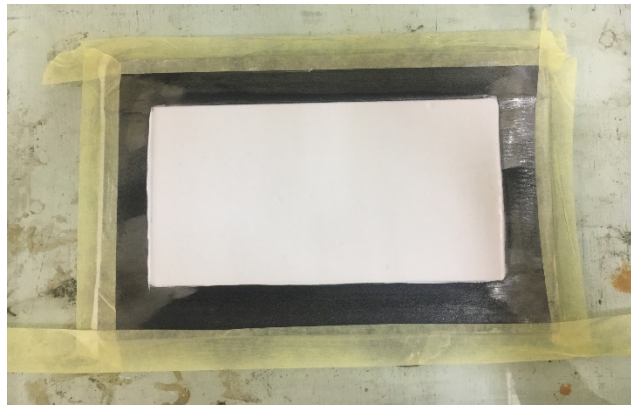


**Figure 5.** The RMP applied on the surface of glass inside the frame (dimensions:  $20 \times 10.4 \times 2.7$  mm).

The mass of the RMP that penetrated ( $M_{pp}$ ) was determined as follows:

$$M_{pp} = M_p - M_0 \quad (2)$$

where

- $M_{pp}$ : mass (in g) of the RMP that penetrated into the surface voids inside the contact surface area (frame/specimen surface), which represented  $113.04 \text{ cm}^2$ .
- $M_p$ : mass of the RMP (in g) deposited on the frame at the interface (frame/specimen surface).
- $M_0$ : mass of the RMP (in g) deposited on the frame at the interface (frame/glass surface);  $M_0 = 103.62 \text{ g}$ .

Knowing the mass of RMP that penetrated into all surface defects, we can then calculate its volume, which represents the volume of the defects. The calculation was made using the following equation:

$$V_{\text{defects}} = \frac{M_{pp}}{\rho} \quad (3)$$

where

- $M_{pp}$  is the mass of RMP that penetrated (g);
- $V_{\text{defects}}$  is the defect volume ( $\text{cm}^3$ );
- $\rho$  is the RMP density ( $1.845 \text{ g/cm}^3$ ).

The percentage of defects by volume was calculated in relation to 100% of the inspected area with the following expression:

$$\text{SDI}(\%) = \frac{V_{\text{defects}}}{V_0} \times 100 \quad (4)$$

where  $V_0$  is the known volume of RMP deposited inside the frame placed on the glass surface (reference medium).

$$V_0 = S \times e \quad (5)$$

where:

- $S$ : is the inner surface area of the frame (contact surface between RMP and the glass surface), which is  $208 \text{ cm}^2$ .
- $e$ : is the thickness of the frame, which is equal to  $2.7 \text{ mm}$ .

### 5. Validation of the SDI (Surface Defect Index) Method: Experiments on Repeatability and Reproducibility

In measurement system analysis (MSA), there are several formulas that are used to quantify the performance and characteristics of a measurement system. These formulas help to quantify different components of measurement variation, such as repeatability and

reproducibility. They are used to assess the quality and reliability of a measurement system. The objective of this part of the study is to validate the accuracy of measurements, reproducibility, and repeatability of the SDI (Surface Defect Index) method. Through rigorous testing and analysis, we aim to establish the method's reliability in measuring defects' volume and evaluating the quality of concrete surfaces efficiently. The validation procedure is founded on key parameters for quantifying surface defects under various conditions using controlled samples. These parameters include their shape, size, depth profile, density, and distribution. This validation process involves a comprehensive assessment of the method's performance considering various factors. We report the accuracy of the measurements at all levels identified in the procedure and cover the repeatability, reproducibility, and accuracy of the measurements.

### 5.1. Specimen Test Preparation, Conditioning, and Test Parameters

Theoretically, this method is capable of quantifying concrete surface defects. The test samples needed to be prepared according to the study's specifications. To obtain repeatability and reproducibility parameters, a series of four (27.5 cm × 17 cm × 2.5 cm) surface specimens were manufactured using plaster. Plaster is a material with an imprint; it is dimensionally stable and offers high precision, as well as detailed definition. Due to the variety of surface defects encountered, the validation of the method would require adaptation to each level of surface defects and evaluation in a case-by-case study. In order to present different surface defects that can affect the appearance, functionality, and durability of structures, surface specimens on which defects with known characteristics were reproduced were manufactured. Defects on specimen surfaces can be defined as ideal in the sense that they are regular and perfectly clean geometric indications. For this purpose, fifteen types of forex texturing patterns with different shapes, sizes, and depths were manufactured, as shown in Figure 6. These patterns were used to create defects on the surface of the molded specimens with well-defined volumes, as shown in Table 2. Each printed defect presented specific characteristics, such as its shape, size, and depth. These features were carefully chosen to ensure a variety of defect configurations that could be studied and evaluated as part of this research.

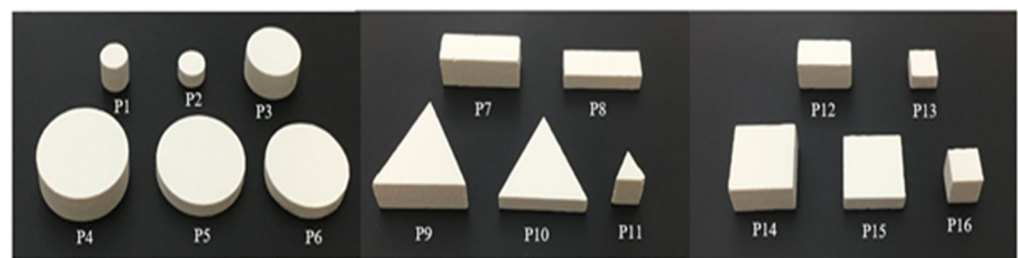


**Figure 6.** List of the texturing patterns.

**Table 2.** Measured volume of the texturing patterns.

Texturing Patterns	P1	P2	P3	P4	P5	P6	P7	P8	P9
Volume (cm <sup>3</sup> )	0.785	0.392	3.14	7.065	3.532	3.065	3	1.5	3.75
Texturing Patterns	P10	P11	P12	P13	P14	P15	P16		
Volume (cm <sup>3</sup> )	1.875	0.4	2	0.5	4	2	1		

### 5.2. The Process of Preparing Test Specimens

After casting the plaster, a powder release agent was sprinkled on the molded surface to facilitate the detachment of the texturing patterns. Once the texturing patterns were well distributed across the surface, a glass plate was placed on the surface with a certain pressure to provide uniform implantation of the texturing patterns and guarantee the perfect flatness of the surface.

The texturing patterns were pre-perforated, allowing a screw to be placed inside subsequently. This operation needed to be performed by carefully retrieving all of the patterns. Once the surface specimens' preparation was completed, the test specimens were exposed to drying in the laboratory until the dimensional stability of the volumes of the defects created was achieved. The main steps in the specimens' preparation are summarized in Figure 7.

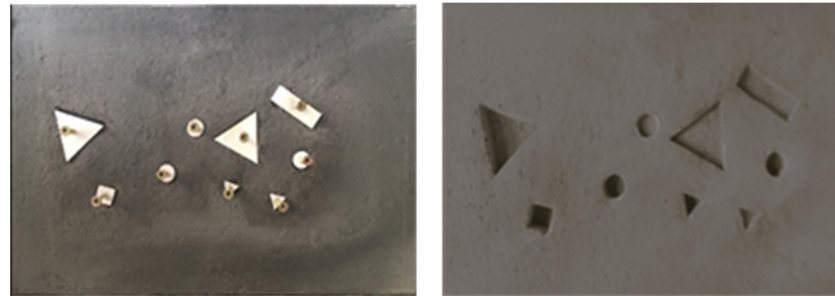


**Figure 7.** Preparation of the defect configurations in the specimens.

Furthermore, to avoid the presence of imperfections induced during the casting process and, thus, to truly isolate the effect of roughness on the tested surfaces, the samples were coated with an epoxy film that allowed for smooth surfaces that were resistant and free from undesirable defects. Only variations in defects found during surface preparation should be considered for quantifying the defect volume, which allowed for the accurate and detailed characterization of the surface profile. The epoxy film also allowed perfect and thorough cleaning of surfaces to facilitate their reuse in repeatability and reproducibility studies.

According to the specifications of the surface defect characteristics, the surface samples were grouped into four types of configurations. These configurations were carefully designed to represent different defect characteristics that can be encountered in real situations. Thus, each sample of configurations allowed for the assessment and study of a specific set of defects based on various defect parameters, such as size, shape, depth, distribution, and density, as follows:

- Configuration C1: (P12, P7, P8, P9, P10, P5, P6, P14) with a theoretical volume of defects equal to  $22.72 \text{ cm}^3$  and a theoretical surface area of defects of  $32.71 \text{ cm}^2$ .
- Configuration C2: (3.P16, P13, 2.P1, 2.P2, P11) with a theoretical volume of defects equal to  $6.25 \text{ cm}^3$  and a theoretical surface area of defects of  $7.54 \text{ cm}^2$ .
- Configuration C3: (P11, P10, P15, P5, 2.P16, 2.P1) with a theoretical volume of defects equal to  $11.37 \text{ cm}^3$  and a theoretical surface area of defects of  $18.78 \text{ cm}^2$ .
- Configuration C4: (P9, P10, P14, P12, P4, P5, P3) with a theoretical volume of defects equal to  $25.36 \text{ cm}^3$  and a theoretical surface area of defects of  $30.77 \text{ cm}^2$ .

Figure 8 shows the appearance of the four surface configurations: C1, C2, C3, and C4. Each surface sample had a specific configuration that encompassed defects of various sizes, lengths, depths, and shapes, covering a wide range of scenarios corresponding to one of the configurations mentioned above. The four configurations reflected the expected variability under the conditions of repeatability and reproducibility and were adapted to the measurements to be made.

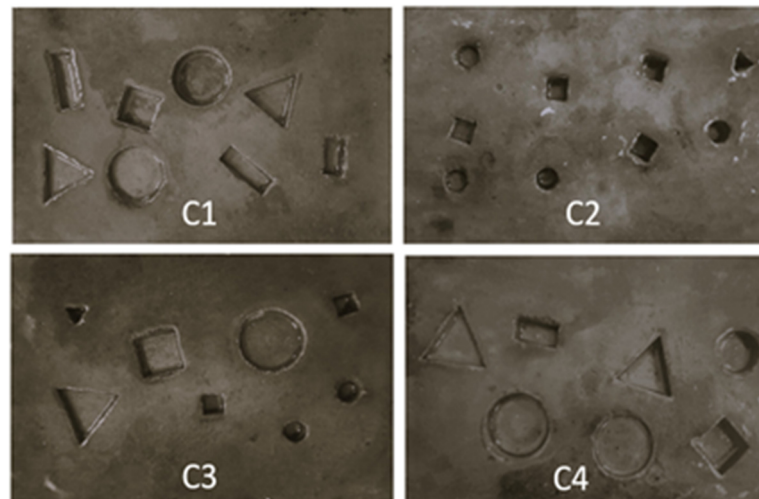


**Figure 8.** View of surface configurations C1 to C4 of the test specimens showing the various defects profiles.

### 5.3. Application of Ready-Mixed Plaster (RMP) and Execution of Measurements

After the preparation of the test samples, the surfaces were subjected to plastering tests, where the ready-mixed plaster (RMP) was applied following the guidelines of the SDI method. The main steps in applying RMP to the surfaces of the test specimens are summarized in Figure 9.

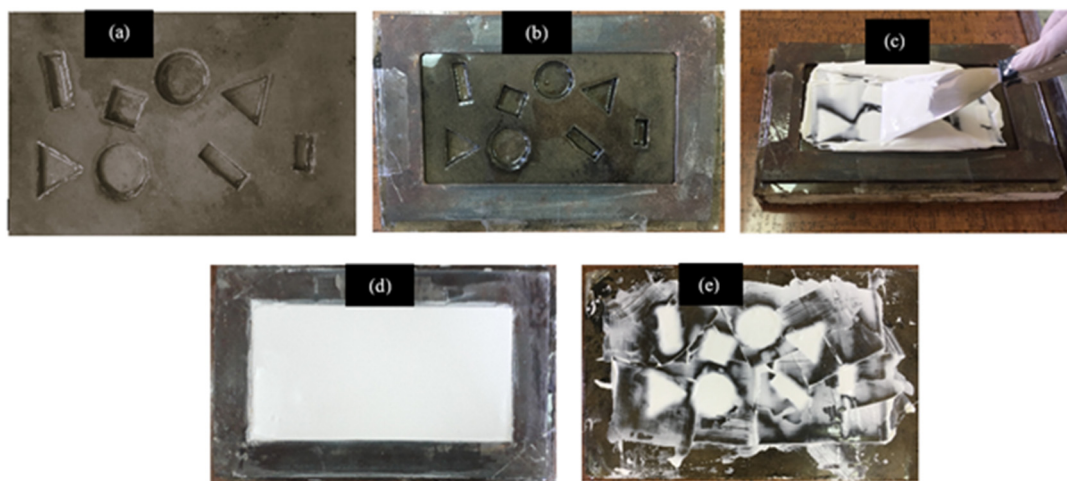


**Figure 9.** Specimen surface in the different steps of the RMP application process: (a) sample surface with various defects; (b) placement of the frame on the surface with all defects grouped inside; (c) application of the RMP on the framed area; (d) filling of the interior of the frame. In (e), all defects were filled after removing the frame and unloading the RMP from it.

The measured ready-mixed plaster masses for each sample were investigated as quantitative variables. These variables are represented as the mean ( $M$ ), standard deviation for repeatability ( $SDr$ ), and standard deviation for reproducibility ( $SDR$ ), along with the corresponding coefficients of variation in repeatability and reproducibility ( $CVr\%$  and  $CVR\%$ ). First, repeatability (within-operator variance) and repeatability variance was assessed as follows: an operator performed four repeated measurements on the same specimen. This represented the variation due to repeated measurements by the same operator on the same specimen.

The formula for calculating the standard deviation for repeatability is

$$SDr = \sqrt{\sum \left( (V_i - \bar{V})^2 / (n - 1) \right)} \tag{6}$$

where  $V_i$  is the  $i$ th measurement,  $\bar{V}$  is the average of all measurements, and  $n$  is the total number of measurements. The coefficient of variation for repeatability (%CVR) is given by

$$CVR\% = (SDr / \bar{V}) \times 100 \tag{7}$$

Next, reproducibility (between-operator variance) or reproducibility variance was assessed as follows: two operators (operators A and B) performed the measurement procedure on four configurations/parts. This represented the variation due to differences between operators.

The formula for calculating the standard deviation for reproducibility is

$$SDR = \sqrt{\sum \left( (V_i - \bar{V})^2 / (k - 1) \right)} \tag{8}$$

where  $V_i$  is the average of measurements by the  $i$ th operator,  $\bar{V}$  is the overall average of all measurements, and  $k$  is the number of operators. The coefficient of variation for reproducibility is given by

$$\%CVR = (SDR / \bar{V}) \times 100 \tag{9}$$

Hence, four surface specimens were measured by two operators with four replications, resulting in a total of 32 conducted experiments.

### 6. Results and Discussion

Tables 3 and 4 summarize the results of the measurements performed by the operators and the different variables calculated in the assessment of repeatability and reproducibility.

**Table 3.** Summary of operators’ results for the different specimens.

		Operator A											
		Specimens											
Measurement		C1			C2			C3			C4		
		Amount of RMP Applied (g)	Defect Volume (cm <sup>3</sup> )	SDI (%)	Amount of RMP Applied (g)	Defect Volume (cm <sup>3</sup> )	SDI (%)	Amount of RMP Applied (g)	Defect Volume (cm <sup>3</sup> )	SDI (%)	Amount of RMP Applied (g)	Defect Volume (cm <sup>3</sup> )	SDI (%)
	1	148.0	24.05	42.82	116.8	7.09	12.62	124.9	11.53	20.53	151.9	26.16	46.58
	2	146.4	23.18	41.27	115.7	6.55	12.62	126.8	12.56	22.36	152.0	26.22	46.69
	3	147.3	23.67	42.15	117.0	7.25	12.91	125.9	12.07	21.49	150.9	25.63	45.64
	4	146.8	23.40	41.66	116.2	6.82	12.14	126.1	12.18	21.69	152.7	26.60	47.36
	Mean	147.12	23.57	41.97	116.42	6.93	12.34	125.92	12.08	21.52	151.87	26.15	46.57
	Theoretical values		22.72	40.45		6.25	11.13		11.37	20.24		25.36	45.16

Table 3. Cont.

		Operator B											
		Specimens											
Measurements		C1			C2			C3			C4		
		Amount of RMP Applied (g)	Defect Volume (cm <sup>3</sup> )	SDI (%)	Amount of RMP Applied (g)	Defect Volume (cm <sup>3</sup> )	SDI (%)	Amount of RMP Applied (g)	Defect Volume (cm <sup>3</sup> )	SDI (%)	Amount of RMP Applied (g)	Defect Volume (cm <sup>3</sup> )	SDI (%)
1		147.5	23.78	42.34	116.0	6.71	11.95	127.4	12.88	22.93	153.6	27.09	48.24
2		148.8	24.49	43.61	115.3	6.33	11.27	126.9	12.62	22.47	151.8	26.11	46.49
3		146.9	23.46	41.77	116.5	6.98	12.43	127.6	12.94	23.04	152.9	26.71	47.56
4		148.8	24.49	43.61	115.5	6.44	11.47	125.5	11.86	21.12	152.1	26.28	46.79
Mean		147.85	24.05	42.83	115.82	6.61	11.78	126.85	12.57	22.39	152.60	26.55	47.27
Theoretical values			22.72	40.45		6.25	11.13		11.37	20.24		25.36	45.16

Table 4. Standard deviation (SDr, SDR) and coefficient of variation (CVr, CVR) of the measurements for each specimen.

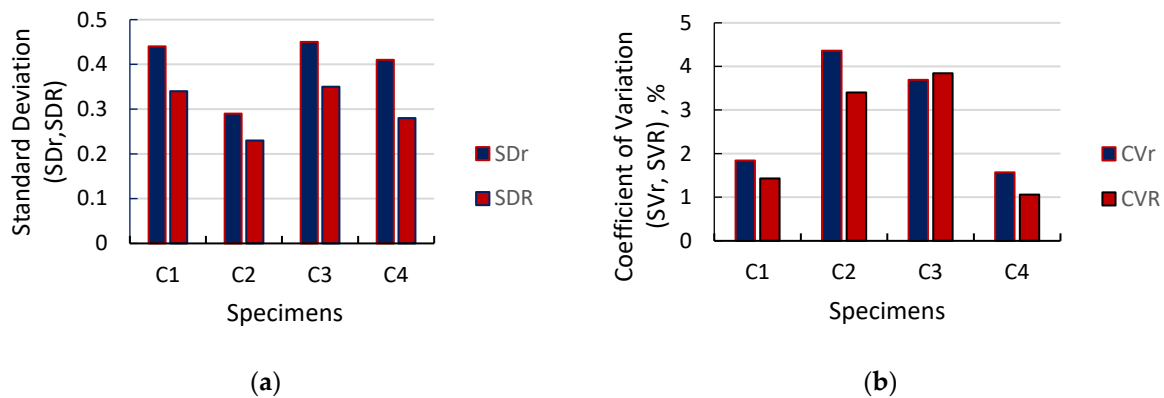
Operators		Specimens			
		C1	C2	C3	C4
A	SDr	0.37	0.30	0.42	0.40
B	SDr	0.51	0.29	0.49	0.43
Mean SDr		0.44	0.29	0.45	0.41
A	SDR	0.34	0.23	0.35	0.28
B	SDR	0.34	0.23	0.35	0.28
A	CVr %	1.57	4.33	3.48	1.53
B	CVr %	2.12	4.39	3.90	1.62
Mean CVr %		1.84	4.36	3.69	1.57
A	CVR %	1.43	3.40	3.84	1.06
B	CVR %	1.43	3.40	3.84	1.06

Figure 10a displays a comparison of the results for the standard deviations for repeatability (SDr) and reproducibility (SDR) involving the different configurations of surface defects, with each surface having a specific theoretical volume of defects. The standard deviations for repeatability (SDr) and reproducibility (SDR) were generally consistent across configurations. A comparison of the results shows that the standard deviation for reproducibility (SDR) was slightly lower than the standard deviation for repeatability (SDr) for each configuration, suggesting that the variability between operators was slightly lower than the variability of repeated measurements by the same operator. The relatively low values indicated good accuracy and greater repeatability and reproducibility in measurements for these configurations.

- Configuration C1: The standard deviations for repeatability and reproducibility were relatively low for this configuration (SDr = 0.44, SDR = 0.34). This suggests high precision and consistency between repeated measurements and across operators.
- Configuration C2: The standard deviations remained low (SDr: 0.29, SDR: 0.23), indicating that even for smaller defect volumes, the measurement method maintained good precision and acceptable repeatability and reproducibility.
- Configuration C3: The standard deviations for repeatability and reproducibility were consistent with those of the previous configurations (SDr: 0.45, SDR: 0.35). The

method maintained its precision, repeatability, and reproducibility for a moderate defect volume.

- Configuration C4: Once again, the standard deviations remained low (SDr: 0.41, SDR: 0.28), suggesting that even for larger defect volumes, the method maintained high precision and satisfactory repeatability and reproducibility.



**Figure 10.** (a) Variations in SDr and SDR; (b) variations in SVr and SVR as affected by various defect configurations, repeated measurements, and operators.

From the comparison results shown in Figure 10b, it is demonstrated that the CVr % (coefficient of variation of repeatability) values were slightly higher than the corresponding CVR % (coefficient of variation of reproducibility) values for all of the specimens. This suggests that the variability in measurements taken by the same operator (CVr) for a specific specimen was slightly higher than the variability observed when different operators measured the same specimen (CVR). The two indicators of variability were nearly identical, implying a high level of measurement reliability. This suggests that the method used to measure these surface specimens demonstrated good repeatability and reproducibility across different configurations of defects.

- Configuration C1 (CVr: 1.84%, CVR: 1.43%): This defect configuration exhibited very low variability, both for measurements repeated by the same operator (CVr) and for measurements between different operators (CVR). The CVr and CVR values were close and low, indicating high consistency and repeatability, as well as reproducibility of measurements. The CVr and CVR values below 5% for this configuration indicate that the measurement method was highly precise and consistent [53–55], suggesting an accurate defect volume assessment for a defect configuration with a relatively larger volume. The measurement method proved to be reliable for assessing a relatively larger defect volume with consistent results.
- Configuration C2 (CVr: 4.36%, CVR: 3.40%): Measurements repeated by the same operator (CVr) displayed slightly higher variability than in Configuration C1. However, the variability between different operators (CVR) was also slightly higher but still acceptable. Although slightly higher than for Configuration C1, the CVr and CVR values were still below 5%, indicating good precision and satisfactory repeatability and reproducibility. Consequentially, despite the smaller defect volume, the method's consistency suggests that it can reliably capture smaller defect sizes.
- Configuration C3 (CVr: 3.69%, CVR: 3.84%): The results were similar to those of Configuration C2, with slightly higher variability values for measurements repeated by the same operator (CVr) and between different operators (CVR). Similarly to the previous configurations, the CVr and CVR values below 5% point to a method with high precision. The consistency of the measurements across the moderate defect volume indicate reliable performance regardless of defect size.
- Configuration C4 (CVr: 1.57%, CVR: 1.06%): This configuration demonstrated variability values similar to those of Configuration C1, with high consistency in measurements

repeated by the same operator (CVr) and between different operators (CVR). Configuration C4 stood out for its exceptional precision and consistency in measurements, showcasing CVr and CVR values that were among the lowest. The stability in the measurements suggests that the method could accurately capture larger defect volumes as well. Despite the larger defect volume, the CVr and CVR values remaining below 5% indicate a method that can handle different defect scales.

In our study, all four defect configurations of the specimen surfaces exhibited very low variability in measurements. The coefficient of variation of repeatability (CVr) and the coefficient of variation of reproducibility (CVR) for each configuration were both below 5%. The small variability indicates that our measurements were consistently close to the mean value for each configuration. This indicates a high level of consistency, repeatability, and reproducibility in our measurements. The relationship between the CVr and CVR values and the theoretical defect volume showcases the robustness and adaptability of our measurement method. The fact that the CVr and CVR values were consistently below 5% across different defect volumes implies that the SDI method is not significantly influenced by the specific defect size.

This consistency enhances the credibility of our results and suggests that the method can reliably assess defect volumes across a range of sizes. The combination of low CVr and CVR values with consistent measurements for various defect configurations and volumes underscores the accuracy, reliability, and versatility of our measurement method in assessing the volume of surface defects in concrete surfaces.

The following are the conclusive outcomes of the validation:

- High precision: The fact that both the CVr and CVR values were below 5% suggests that our measurement method is highly precise. The small variability indicates that our measurements were consistently close to the mean value for each configuration.
- Reliability: The consistency across all defect configurations suggests that our measurement method is robust and reliable. The method was not significantly affected by the specific features of each configuration.
- Consistent performance: Regardless of the specific characteristics of the surface defects, our measurements remained stable, repeatable, and reproducible. This implies that our method was capable of producing reliable results under various conditions.
- Validation findings: The low variability values are indicative of a well-controlled measurement process. This provides confidence that the method can be effectively used to assess the surface defect volume in concrete samples.

Consequently, based on the results gathered in Table 2, a correlation between the experimental and theoretical measurements of the defect volume is evident. From the data in Figure 11a, there is a strong positive linear correlation and high agreement ( $R^2 = 0.9968$ ) between the experimental measurements of the defect volume by both operators and the theoretical values of the defect volume for each configuration. This is an extremely favorable result that confirms the validity and high accuracy of the experimental measurements with respect to the theoretical values of the defect volume. In addition, in Figure 11b, an extremely strong positive correlation ( $R^2 = 0.9968$ ) is shown between the experimental index and the theoretical index, suggesting that the experimental SDI accurately reflects variations relative to the theoretical SDI. The experimental SDI is a robust indicator for evaluating the conformity of experimental measurements with theoretical measurements of defect volume.

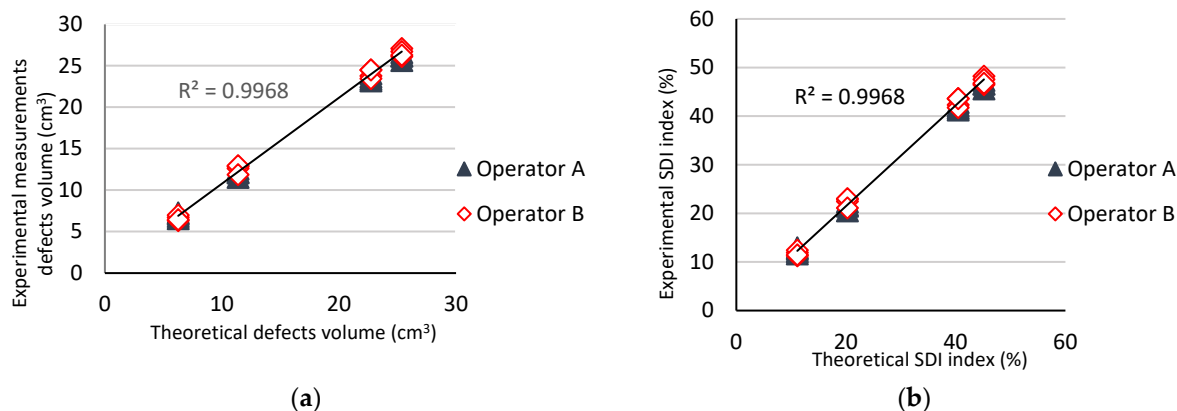


**Figure 11.** Correlation between the experimental and theoretical values: (a) defect volume and (b) SDI.

#### *Surface Quality Evaluation with the SDI of the Controlled Specimens*

In order to compare the variability at the different levels of defects in this study, the average values of the experimental SDI for each of the controlled samples were calculated. The individual SDI of each of the configurations is presented in Table 5 with the theoretical values (comprising previous data from controlled samples).

**Table 5.** Theoretical values and experimental average values of the SDI for each configuration.

Configuration	Theoretical Volume of Defects (cm <sup>3</sup> )	Theoretical Surface Area of Defects (cm <sup>2</sup> )	SDI (%)	Experimental Volume of Defects * (cm <sup>3</sup> )	SDI * (%)
C1	22.72	32.71	40.45	23.81	42.4
C2	6.25	7.54	11.13	6.77	12.05
C3	11.37	18.78	20.24	12.32	21.94
C4	25.36	30.77	45.16	26.35	46.92

(\*) Mean value.

The advantage of the SDI is that it quantifies the defect volume by considering both the spatial extent (surface area) and the depth of defects. This provides a more comprehensive assessment of surface quality, accounting for defects that may not be immediately visible at the surface but can still impact long-term performance. For example, honeycombs, deep cracks, and bugholes in concrete may indicate durability problems that may not necessarily be detected through surface assessment alone.

The quantification of the defect volume often has a stronger correlation with material durability than the quantification of the defect surface area. Defects that penetrate deep into a material typically have a more significant impact on durability. Although Configuration C1 had a larger total defect area than that of Configuration C4 (estimated at 32.71 cm<sup>2</sup> and 30.77 cm<sup>2</sup>, respectively), the SDI was lower for Configuration C1, with a value equal to 42.4 (42.4% of the volume occupied by defects) compared to the volume of defects occupied by Configuration C4, which was estimated at 46.92%. This was due to the greater depth of defects in C4, which had a more significant impact on the surface quality. In other words, even though C1 had a greater defect surface area, the defects were less deep, resulting in a lower SDI.

This comparison highlights that the SDI takes into account the depth of defects, in addition to the surface area, when assessing surface quality. In this case, it demonstrates that the depth of defects can be a determining factor in the quality of a surface.

That is, the quality of the sample surfaces is closely related to the defect volume. Actually, Figure 12 demonstrates an excellent correlation between this index and the volume of defects when the surface quality is assessed through the SDI, suggesting that

the measurements of the SDI and the volume of defects are consistent and reliable, which enhances the validity and reliability of this study's results.

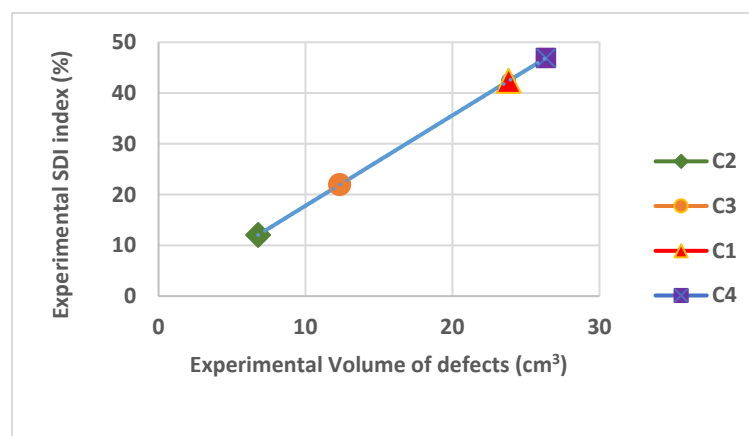


**Figure 12.** Relationship between the volume of defects (surface area, depth) and the SDI.

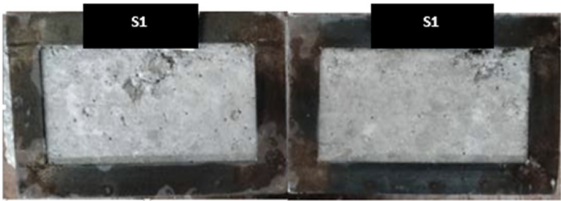
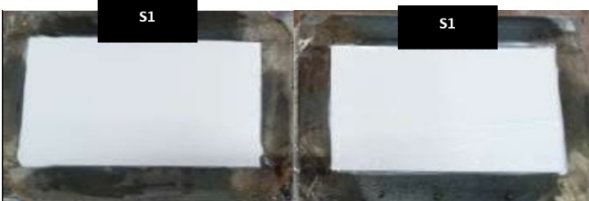
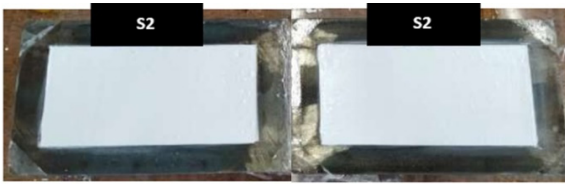
This strong linear relationship implies a direct dependence between the SDI and the volume of defects. In other words, as the volume of defects increases, the SDI increases proportionally. For example, if the surface defects increase in surface area or depth, their volume will also increase proportionally, which reflects the linear relationship between the SDI and the volume of defects. The observed linear relationship between the SDI and the experimental volume of defects suggests consistency in measurements and a direct correlation between surface quality and the volume of defects and, consequently, between surface quality and the SDI. These findings are consistent with previous studies [5,6], which revealed a strong relationship between the surface area, the depth of the defects, and the quality of surfaces. These defects may allow the accumulation of contaminant agents and promote the agglomeration of microorganisms that can compromise the structural integrity of the concrete and detract from its aesthetic appearance.

According to these criteria, the SDI can be employed to classify the levels of surface quality. These classifications provide an insight into the quality of the sample surfaces, where a low SDI indicates a higher surface quality due to the low defect volume, while a high index is associated with lower surface quality due to the high defect volume. Therefore, Configuration C2, with the lowest SDI, represents the highest quality, while Configuration C4, with the highest index, indicates the lowest surface quality.

## 7. Application Examples of the SDI on Real Concrete Surfaces

The index proposed in this study underwent practical application on real concrete surfaces to assess its potential utility and the accuracy of its defect quantification capabilities. The selection of specific examples for the application of the SDI was methodically determined, as depicted in Table 6. Each chosen example involved careful consideration of different defect rates and represented a distinct quality of concrete surfaces, ranging from pronounced defects to minor imperfections. Specifically, the defects ranged from the most pronounced on surface S1 to moderate defects on surface S2 and minimal defects on surface S3. This selection was intended to provide a pertinent assessment of the SDI's versatility across different conditions of concrete surfaces. Two frames were positioned on samples of concrete surfaces. The frames delineated specific areas affected by surface defects for calculating the percentage of the defects' volume.

**Table 6.** SDI values and visual representations for various concrete surfaces.

Concrete Surfaces Examined	Application of the RMP on the Framed Area	SDI (%)
		68.58%
		15.03%
		1.61%

After the application of the RMP to the concrete surfaces inside both frames, the results displayed a significant variation. Surface indices of 68.58%, 15.03%, and 1.61% were obtained for surfaces S1, S2, and S3, respectively, reflecting the differing levels of defects encountered. This variation underscores the sensitivity of the index to nuances in surface quality. The index of 15.03% represents a surface with characteristics distinct from those with higher or lower indices. This range of results highlights the SDI's sensitivity in discerning and quantifying defects at different levels of defect severity, showcasing its effectiveness in capturing the variability in concrete surface conditions.

The results reveal a direct correlation between the SDI values and the quality of the concrete surfaces. A higher index value (68.58%) corresponds to a surface with a higher volume of defects, suggesting potentially lower surface quality in terms of durability, while a lower value (1.61%) indicates a surface with a minimal defect volume, suggesting higher surface quality and, by extension, increased durability of the concrete. Notably, the surface with an index of 15.03% represented a moderate level of defects, indicating a moderate level of surface quality. This direct relationship showcases the efficacy of the SDI as a quantitative measure for defect characterization. The results specify the SDI as a valuable tool for distinguishing between varying levels of surface quality, contributing to accurate defect quantification and objective quality evaluation. By quantifying defects accurately, the SDI provides a meaningful approach to predicting the strength and durability of concrete, thus supporting more reliable durability assessments in the construction industry.

## 8. Conclusions

In this study, a novel Surface Defect Index (SDI) method is proposed to quantify the volume occupied by various types of defects and reveal their positions and infiltration within concrete surfaces. This method establishes a quantitative survey of defects in terms of surface area and depth, enabling a comprehensive evaluation of concrete surface quality.

One of the strengths of the proposed method lies in the use of controlled samples featuring various defect configurations, which allowed us to create a rigorous testing environment where we could precisely assess the method's effectiveness. Using these samples, SDIs were obtained for each surface, providing concrete results that underscore

the relevance of the method. The validation of the measurement method demonstrated its high precision, reliability, and consistent performance. These validation findings instill confidence in the ability of the method to effectively assess the surface defect volume in concrete samples.

The correlation between the SDI and the defect volume in the various defect configurations was investigated. Strongly correlated with the defect volume variability, the SDI provides coherent measurements of the defect volume for a large range of sizes. A strong positive linear correlation and high agreement ( $R^2 = 0.9968$ ) were observed between the experimental volume and effective volume of defects. Therefore, the SDI can be a robust indicator for quantifying the defect volume over a wide variety of defect scales. The method effectively evaluated the levels of quality using the SDI; this was demonstrated by the strong relationship between this index and the volume of defects.

The effectiveness and reliability of our measurement method make it a valuable tool for assessing the quality of concrete surfaces with a high degree of precision and consistency. The SDI was tested across a diverse array of real conditions of concrete surfaces, confirming its applicability and reliability in concrete quality assessment.

Furthermore, the logic-based evaluation, which was based on a new Surface Defect Quantification Index, was efficient in classifying the final quality of concrete surfaces according to the volume occupied by all defects on the surfaces. The surface area and the maximum depth of defects were used as parameters for the evaluation and classification of surfaces in terms of their durability attributes. These classifications provide insights into the quality of sample surfaces; hence, surfaces with higher SDI values are of better quality, while the surfaces with the highest SDI values are of lower quality. Therefore, the Surface Defect Index can serve as a valuable indicator for evaluating the susceptibility of a material to the penetration of aggressive substances. It can be regarded as an indicator of the durability of concrete, its performance, and its service life. Through early detection and remediation of surface defects in concrete, it is feasible to enhance the durability and lifetime of concrete structures, consequently relieving the need for costly future repairs and maintenance.

Contrary to the limitations associated with several methods for the assessment of the quality of concrete surfaces, the developed method offers several advantages. Firstly, its simplicity and ease of implementation make it accessible to a wider range of users without requiring specialized expertise. Secondly, the method significantly reduces time requirements, particularly for large surfaces or those with numerous defects, enabling rapid assessments even in time-sensitive conditions compared with referenced methods [11,18]. Additionally, its high-resolution capabilities allow for the accurate detection and quantification of small defects or fine details on concrete surfaces, providing comprehensive and detailed evaluations. Moreover, the SDI method is less dependent on human judgment, thus reducing the subjectivity in the final results and ensuring consistent and reliable results regardless of variations among inspectors and the complexity of defects.

Overall, these advantages position the developed method as a practical and efficient solution for evaluating concrete surface defects, addressing the challenges associated with various methods and enhancing the assessment process. Further investigation could involve a parametric and comparative study with other current methods. While the current study has provided valuable insights into the effectiveness of the proposed method for evaluating concrete surfaces, future research could focus on extending the application of this method by exploring its applicability to different contexts for meaningful applications in the construction and civil engineering industries and in other areas of application.

**Author Contributions:** Conceptualization: F.Z.B., S.E.B., A.C., C.B., T.T.N., E.H.K. and S.C.; methodology: F.Z.B., S.E.B., T.T.N., C.B. and S.C.; software: F.Z.B., S.E.B., A.C., C.B., T.T.N., E.H.K. and S.C.; validation: All authors; formal analysis: All authors; investigation: All authors; resources: F.Z.B., S.E.B., T.T.N. and C.B.; data curation: All authors; writing—original draft preparation: F.Z.B., S.E.B., A.C. and T.T.N.; writing—review and editing: F.Z.B. and C.B.; visualization: All authors; supervision: F.Z.B., S.E.B., A.C., C.B., T.T.N., E.H.K. and S.C.; project administration: All authors;

funding acquisition: All authors. All authors have read and agreed to the published version of the manuscript.

**Funding:** This research received no external funding.

**Institutional Review Board Statement:** Not applicable.

**Informed Consent Statement:** Not applicable.

**Data Availability Statement:** The data presented in this study are available on request from the corresponding author. The data are not publicly available due to privacy.

**Conflicts of Interest:** The authors declare no conflicts of interest.

## References

- Sadowski, Ł.; Popek, M.; Czarnecki, S.; Mathia, T.G. Morphogenesis in solidification phases of lightweight concrete surface at early ages. *Constr. Build. Mater.* **2017**, *148*, 96–103. [CrossRef]
- Czarnecki, S.; Sadowski, Ł. Morphological properties of the cement skin: Understanding the effect of contact with formwork. *Case Stud. Constr. Mater.* **2022**, *16*, e01007. [CrossRef]
- Martínez-Ramírez, S.; Thompson, G. Dry and wet “deposition” studies of the degradation of cement mortars. *Mater. Construcción* **1998**, *48*, 15–31. [CrossRef]
- Ho, D.; Chirgwin, G.J. A performance specification for durable concrete. *Constr. Build. Mater.* **1996**, *10*, 375–379. [CrossRef]
- Ozkul, T.; Kucuk, I. Design and optimization of an instrument for measuring bughole rating of concrete surfaces. *J. Frankl. Inst.* **2011**, *348*, 1377–1392. [CrossRef]
- Miller, S.A.; Horvath, A.; Monteiro, P.J.; Ostertag, C.P. Greenhouse gas emissions from concrete can be reduced by using mix proportions, geometric aspects, and age as design factors. *Environ. Res. Lett.* **2015**, *10*, 114017. [CrossRef]
- Thompson, M. Blowholes in Concrete Surface. *Concrete* **1969**, *3*, 64–660.
- Kwasny, J.; Sonebi, M.; Plasse, J.; Amziane, S. Influence of rheology on the quality of surface finish of cement-based mortars. *Constr. Build. Mater.* **2015**, *89*, 102–109. [CrossRef]
- Yao, G.; Wei, F.; Yang, Y.; Sun, Y. Detection of Bughole on Concrete Surface with Convolutional Neural Network. In Proceedings of the 2019 4th International Conference on Control, Robotics and Cybernetics (CRC), Tokyo, Japan, 27–30 September 2019; pp. 184–188.
- Zhu, Z.; Brilakis, I. Machine vision-based concrete surface quality assessment. *J. Constr. Eng. Manag.* **2010**, *136*, 210–218. [CrossRef]
- Benito Saorin, F.J.; Miñano Belmonte, I.; Parra Costa, C.; Rodriguez Lopez, C.; Valcuende Paya, M. QSI methods for determining the quality of the surface finish of concrete. *Sustainability* **2018**, *10*, 931. [CrossRef]
- Kaufmann, N. Das sandflächenverfahren. *Straßenbautechnik* **1971**, *24*, 131–135.
- Yu, S.-N.; Jang, J.-H.; Han, C.-S. Auto inspection system using a mobile robot for detecting concrete cracks in a tunnel. *Autom. Constr.* **2007**, *16*, 255–261. [CrossRef]
- Laofor, C.; Peansupap, V. Defect detection and quantification system to support subjective visual quality inspection via a digital image processing: A tiling work case study. *Autom. Constr.* **2012**, *24*, 160–174. [CrossRef]
- Schjodt, R. *CIB Working Commission W29, Tolerances on Blemishes of Concrete*; Norwegian Building Research Institute: Oslo, Norway, 1973; p. 17.
- Wei, F.; Yao, G.; Yang, Y.; Sun, Y. Instance-level recognition and quantification for concrete surface bughole based on deep learning. *Autom. Constr.* **2019**, *107*, 102920. [CrossRef]
- Pushpakumara, B.J.; Silva, S.D.; Silva, G.S.D. Visual inspection and non-destructive tests-based rating method for concrete bridges. *Int. J. Struct. Eng.* **2017**, *8*, 74–91. [CrossRef]
- Majchrowski, R.; Grzelka, M.; Wieczorowski, M.; Gapiński, B. Large area concrete surface topography measurements using optical 3D scanner. *Metrol. Meas. Syst.* **2015**, *22*, 565–576. [CrossRef]
- Concrete International Board—Commission W29. CIB Report n. 24: Tolerances on Blemishes of Concrete. 2003. Available online: <https://www.irbnet.de/daten/iconda/06059000983.pdf> (accessed on 1 April 2024).
- Chermant, J.-L. Why automatic image analysis? An introduction to this issue. *Cem. Concr. Compos.* **2001**, *23*, 127–131. [CrossRef]
- Coster, M.; Chermant, J.-L. Image analysis and mathematical morphology for civil engineering materials. *Cem. Concr. Compos.* **2001**, *23*, 133–151. [CrossRef]
- Abudayyeh, O.; Al Bataineh, M.; Abdel-Qader, I. An imaging data model for concrete bridge inspection. *Adv. Eng. Softw.* **2004**, *35*, 473–480. [CrossRef]
- Ince, T. Unsupervised classification of polarimetric SAR image with dynamic clustering: An image processing approach. *Adv. Eng. Softw.* **2010**, *41*, 636–646. [CrossRef]

24. Chen, Z.; Hutchinson, T.C. Image-based framework for concrete surface crack monitoring and quantification. *Adv. Civ. Eng.* **2010**, *2010*, 215295. [[CrossRef](#)]
25. Lemaire, G.; Escadeillas, G.; Ringot, E. Evaluating concrete surfaces using an image analysis process. *Constr. Build. Mater.* **2005**, *19*, 604–611. [[CrossRef](#)]
26. Liu, B.; Yang, T. Image analysis for detection of bugholes on concrete surface. *Constr. Build. Mater.* **2017**, *137*, 432–440. [[CrossRef](#)]
27. Yoshitake, I.; Maeda, T.; Hieda, M. Image analysis for the detection and quantification of concrete bugholes in a tunnel lining. *Case Stud. Constr. Mater.* **2018**, *8*, 116–130. [[CrossRef](#)]
28. Czarnecki, S.; Hoła, J. Evaluation of the height 3D roughness parameters of concrete substrate and the adhesion to epoxy resin. *Int. J. Adhes. Adhes.* **2016**, *67*, 3–13.
29. Oh, J.-K.; Jang, G.; Oh, S.; Lee, J.H.; Yi, B.-J.; Moon, Y.S.; Lee, J.S.; Choi, Y. Bridge inspection robot system with machine vision. *Autom. Constr.* **2009**, *18*, 929–941. [[CrossRef](#)]
30. Belmonte, I.M.; Saorin, F.J.B.; Costa, C.P.; Paya, M.V. Quality of the surface finish of self-compacting concrete. *J. Build. Eng.* **2020**, *28*, 101068. [[CrossRef](#)]
31. Dorafshan, S.; Thomas, R.J.; Maguire, M. Comparison of deep convolutional neural networks and edge detectors for image-based crack detection in concrete. *Constr. Build. Mater.* **2018**, *186*, 1031–1045. [[CrossRef](#)]
32. Santhi, B.; Krishnamurthy, G.; Siddharth, S.; Ramakrishnan, P.K. Automatic detection of cracks in pavements using edge detection operator. *J. Theor. Appl. Inf. Technol.* **2012**, *36*, 199–205.
33. Li, G.; Ju, Y. Novel approach to pavement cracking detection based on morphology and mutual information. In Proceedings of the 2010 Chinese Control and Decision Conference, Xuzhou, China, 26–28 May 2010; pp. 3219–3223.
34. Wu, G.; Sun, X.; Zhou, L.; Zhang, H.; Pu, J. Research on crack detection algorithm of asphalt pavement. In Proceedings of the 2015 IEEE International Conference on Information and Automation, Lijiang, China, 8–10 August 2015; pp. 647–652.
35. LeCun, Y.; Bottou, L.; Bengio, Y.; Haffner, P. Gradient-based learning applied to document recognition. *Proc. IEEE* **1998**, *86*, 2278–2324. [[CrossRef](#)]
36. Ciregan, D.; Meier, U.; Schmidhuber, J. Multi-column deep neural networks for image classification. In Proceedings of the 2012 IEEE Conference on Computer Vision and Pattern Recognition, Providence, RI, USA, 16–21 June 2012; pp. 3642–3649.
37. He, K.; Zhang, X.; Ren, S.; Sun, J. Spatial pyramid pooling in deep convolutional networks for visual recognition. *IEEE Trans. Pattern Anal. Mach. Intell.* **2015**, *37*, 1904–1916. [[CrossRef](#)] [[PubMed](#)]
38. Krizhevsky, A.; Sutskever, I.; Hinton, G.E. Imagenet classification with deep convolutional neural networks. *Commun. ACM* **2017**, *60*, 84–90. [[CrossRef](#)]
39. Shu, J.; Li, W.; Zhang, C.; Gao, Y.; Xiang, Y.; Ma, L. Point cloud-based dimensional quality assessment of precast concrete components using deep learning. *J. Build. Eng.* **2023**, *70*, 106391. [[CrossRef](#)]
40. Qian, C.; Du, W. Analysis method of apparent quality of fair-faced concrete based on convolutional neural network machine learning. *J. Build. Eng.* **2023**, *80*, 108154. [[CrossRef](#)]
41. Zhang, W.; Wang, R.; Chen, X.; Jia, D.; Zhou, Z. Systematic assessment method for post-earthquake damage of regional buildings using adaptive-network-based fuzzy inference system. *J. Build. Eng.* **2023**, *78*, 107682. [[CrossRef](#)]
42. Zhang, L.; Yang, F.; Zhang, Y.D.; Zhu, Y.J. Road crack detection using deep convolutional neural network. In Proceedings of the 2016 IEEE International Conference on Image Processing (ICIP), Phoenix, AZ, USA, 25–28 September 2016; pp. 3708–3712.
43. Cha, Y.J.; Choi, W.; Büyüköztürk, O. Deep learning-based crack damage detection using convolutional neural networks. *Comput.-Aided Civ. Infrastruct. Eng.* **2017**, *32*, 361–378. [[CrossRef](#)]
44. Zhang, A.; Wang, K.C.; Fei, Y.; Liu, Y.; Tao, S.; Chen, C.; Li, J.Q.; Li, B. Deep learning-based fully automated pavement crack detection on 3D asphalt surfaces with an improved CrackNet. *J. Comput. Civ. Eng.* **2018**, *32*, 04018041. [[CrossRef](#)]
45. Wang, K.C.; Zhang, A.; Li, J.Q.; Fei, Y.; Chen, C.; Li, B. *Deep Learning for Asphalt Pavement Cracking Recognition Using Convolutional Neural Network*; ASCE–Airfield and Highway Pavements: Reston, VA, USA, 2017; pp. 166–177.
46. Chen, F.-C.; Jahanshahi, M.R. NB-CNN: Deep learning-based crack detection using convolutional neural network and Naïve Bayes data fusion. *IEEE Trans. Ind. Electron.* **2017**, *65*, 4392–4400. [[CrossRef](#)]
47. Gummerson, R.; Hall, C.; Hoff, W. Water movement in porous building materials—II. Hydraulic suction and sorptivity of brick and other masonry materials. *Build. Environ.* **1980**, *15*, 101–108. [[CrossRef](#)]
48. Hall, C. Water sorptivity of mortars and concretes: A review. *Mag. Concr. Res.* **1989**, *41*, 51–61. [[CrossRef](#)]
49. Aïssoun, B.; Khayat, K.; Gallias, J.-L. Variations of sorptivity with rheological properties of concrete cover in self-consolidating concrete. *Constr. Build. Mater.* **2016**, *113*, 113–120. [[CrossRef](#)]
50. Sosoro, M. Transport of organic fluids through concrete. *Mater. Struct.* **1998**, *31*, 162–169. [[CrossRef](#)]
51. Yio, M.; Wong, H.; Buenfeld, N. 3D pore structure and mass transport properties of blended cementitious materials. *Cem. Concr. Res.* **2019**, *117*, 23–37. [[CrossRef](#)]
52. Zhou, C.; Li, K.; Pang, X. Geometry of crack network and its impact on transport properties of concrete. *Cem. Concr. Res.* **2012**, *42*, 1261–1272. [[CrossRef](#)]
53. Joubert, J.W.; Meintjes, S. Repeatability & reproducibility: Implications of using GPS data for freight activity chains. *Transp. Res. Part B Methodol.* **2015**, *76*, 81–92.

54. Healy, S.; Wallace, M. Gage repeatability and reproducibility methodologies suitable for complex test systems in semi-conductor manufacturing. *Six Sigma Proj. Pers. Exp.* **2011**, *8*, 153–170.
55. Cepova, L.; Kovacikova, A.; Cep, R.; Klaput, P.; Mizera, O. Measurement system analyses–Gauge repeatability and reproducibility methods. *Meas. Sci. Rev.* **2018**, *18*, 20–27. [[CrossRef](#)]

**Disclaimer/Publisher’s Note:** The statements, opinions and data contained in all publications are solely those of the individual author(s) and contributor(s) and not of MDPI and/or the editor(s). MDPI and/or the editor(s) disclaim responsibility for any injury to people or property resulting from any ideas, methods, instructions or products referred to in the content.